DESIGNING CONFORMAL COOLING CHANNELS FOR TOOLING

Xiaorong Xu, Emanuel Sachs, Samuel Allen, Michael Cima

MIT
Cambridge, MA 02139

Contact:
Emanuel Sachs
MIT
(617) 253-5381
sachs@mit.edu
77 Mass Ave
Cambridge, MA 02139
Rm 35-134

Abstract

SFF technologies have demonstrated the potential to produce tooling with cooling channels which are conformal to the molding cavity. 3D Printed tools with conformal cooling channels have demonstrated simultaneous improvements in production rate and part quality as compared with conventional production tools. Conformal Cooling lines of high performance and high complexity can be created, thus presenting a challenge to the tooling designer. This paper presents a systematic, modular, approach to the design of conformal cooling channels. Recognizing that the cooling is local to the surface of the tool, the tool is divided up into geometric regions and a channel system is designed for each region. Each channel system is itself modeled as composed of cooling elements, typically the region spanned by two channels. Six criteria are applied including; a transient heat transfer condition which dictates a maximum distance from mold surface to cooling channel, considerations of pressure and temperature drop along the flow channel and considerations of strength of the mold. These criteria are treated as constraints and successful designs are sought which define windows bounded by these constraints. The methodology is demonstrated in application to a complex core and cavity for injection molding.

1. Introduction

1.1 Motivation

The cooling of injection molding tooling is crucial to the performance of the tooling influencing both the rate of the process and the resulting quality of the parts produced. However, cooling line design and fabrication has been confined to relatively simple configurations primarily due to the limits of the fabrication methods used to make tools, but also due to the lack of a design methodology appropriate for cooling lines.

For many years mold designers have been struggling for the improvement of the cooling system performance, despite the fact that the cooling system complexity is physically limited by the fabrication capability of the conventional tooling methods. Different methods such as the helical channels, the baffled hole system, the spiral plug system and the heat-pipes have been developed for the uniform and efficient cooling of the part [2]. Some mold manufacturers such as Innova built tools with conformal cooling effect by stacking slices of the tool layer by layer with cooling channels milled on each layer. Other manufacturers such as CITO Products Inc. developed the pulse cooling technique for better control of the mold temperature in order to reduce the energy consumption and enhance uniform cooling condition.

The emergence of Solid Freeform Fabrication (SFF) processes offers injection mold manufacturers new degrees of freedom in mold tooling. The SFF processes are additive processes that construct 3D objects by incrementally building up cross sectional layers of arbitrary complex shapes converted from CAD models. Typical SFF processes include stereolithography, selective laser sintering, three dimensional printing, solid ground curing, laminated object manufacturing, etc. [23]. The ability to fabricate 3D features with almost arbitrary complexity makes these processes extremely useful for fabricating parts and tools that cannot be practically made by other techniques. One example of the applications is to fabricate complex cooling channels inside injection molds in order to improve the uniformity of cooling. The 3D Printing Lab at MIT has been participating in the injection molding tooling project for several years [24, 25, 26]. The industrial application of 3D Printed tools with serpentine conformal cooling channels built inside have achieved the simultaneous improvement of the cycle time by 15% and the part distortion by 9% [26]. With the manufacturing flexibility offered by SFF processes such as 3D Printing, more complex cooling channel systems such as that shown in Figure 1b can be fabricated for the further improvement of the cooling performance.

The emergence of new processes that can be used to create tools with conformal cooling channels placed with almost arbitrary complexity not only offers the designer new degrees of freedom in the design of injection molding tools but also simplifies the methodology used to design cooling channels. The work discussed in this paper seeks to develop a methodology for the design of cooling channels that both simplifies the design and results in substantially improved performance. As you will see from the paper this methodology makes the design of complex cooling channel system for the inserts such as that shown in Figure 1b a handy work.

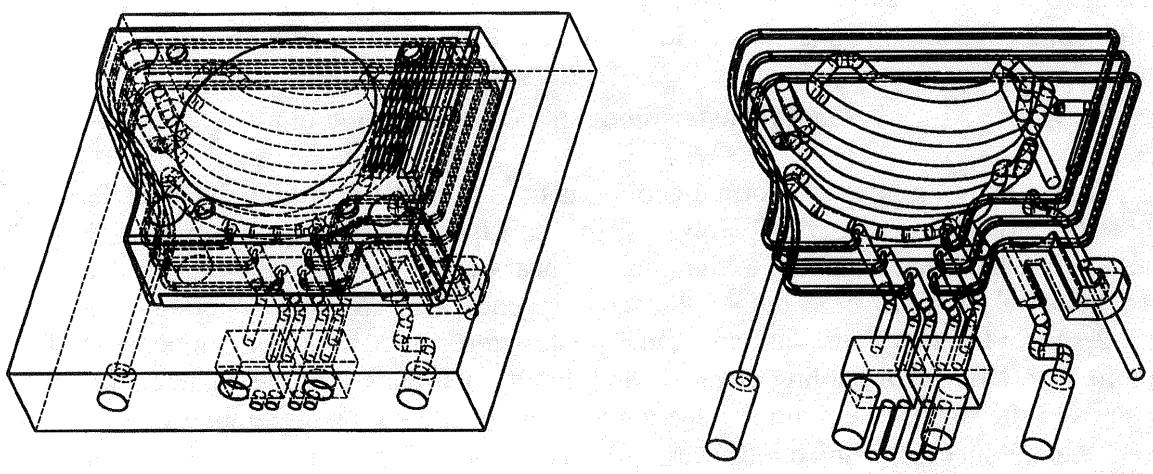

Figure 1. Left: solid model of the core insert with conformal cooling channels built inside. Right: solid model for the conformal cooling channel set

1.2 Related Work

Before the scientific analysis was introduced into injection molding, the design of the mold cooling system was dominated by designers' experience and simple formula [1-4]. It is not until early 80's that the mold cooling simulation was paid more and more attention. Different methods were proposed to predict the temperature field for the mold and the part during the cooling stage [5-14]. The cooling related quality issues such as residual stress, shrinkage and warpage were also addressed in [15-22]. Among those simulation algorithms, an iterative hybrid scheme proposed by Cornell Injection Molding Program (CIMP) became a standard scheme for mold cooling analysis due to its computational efficiency [8-12]. Today most of the mold design packages such as C-MOLD are equipped with this analysis scheme. This scheme treats the plastic part as one-dimensional transient heat transfer and the mold as three-dimensional heat transfer. The periodic transient mold temperature field within an injection cycle is separated into a quasi-steady component and a time–varying component. The quasi-steady component reflecting the cycle–averaged temperature field is obtained by solving the Laplace equation for the entire mold using the boundary element method. The solution is then used as the boundary for 1D part temperature field. The iterative reference between the boundary element solution of the cycle-averaged mold temperature field and the finite difference solution of the part temperature field continues until a steady temperature boundary is achieved at the mold-part interface. Compared with the finite element simulation that needs to calculate the internal nodes, the hybrid scheme discussed above significantly reduces the computational time because only the boundary nodes are considered for obtaining the cycle-averaged mold temperature field.

The emerging techniques for freeform fabrication of the injection molding tools place a new challenge to the mold design and analysis strategy due to the increased complexity in cooling channel geometry. This situation motivates us to develop a systematic tool for conformal cooling line design. Compared with the existing cooling analysis software, the methodology

discussed in this paper builds a synthesis tool instead of an analysis tool for the design of the complex conformal cooling channels which take the full advantage of SFF processes.

2. Heat transfer model for conformal cooling

As the name implies, conformal cooling is used to signify cooling channels that conform to the surface of the mold cavity. However, in this paper, the term "conformal cooling" has a further significance that is related to the transient heat transfer within the mold. When a mold is started up it takes some time before the mold reaches a steady state operating temperature. Figure 2 shows the mold surface temperature histories recorded by the thermocouples for both the mold with conformal cooling channels and that with straight cooling channels [24]. As one can see from the figure, the mold surface temperature of the core with straight cooling channels tracked over 25 successive injections starting from the coolant temperature of 12° C and reaching a cycle average steady state temperature of approximately 55° C. However, if the cooling lines are placed very close and conformal to the mold surface the steady state condition is reached very quickly. As illustrated in Figure 2 the cycle average temperature of a conformally cooled core reaches its steady state value after one injection cycle. Our operational definition of conformal cooling then is that the cycle average temperature reaches its steady state value within one injection cycle. As shown by experiments, the difference of the mold surface temperature profiles we just discussed above significantly effects the part quality and productivity.

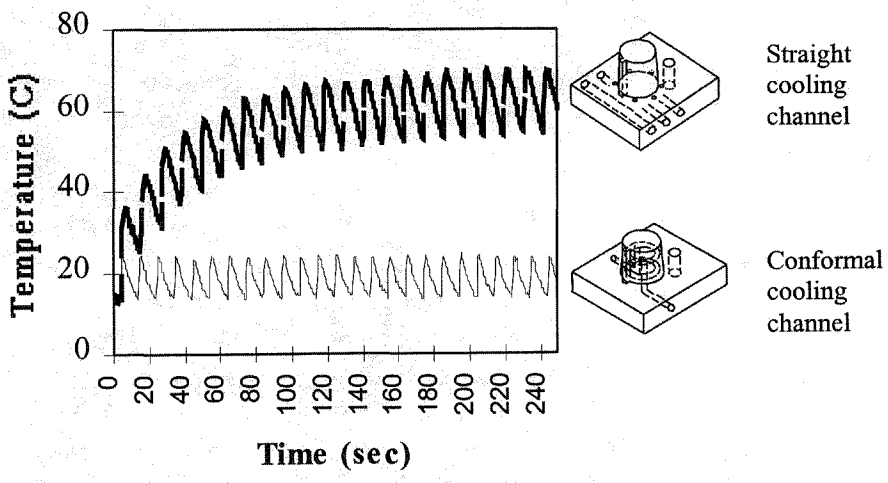

Figure 2. Comparison of mold surface temperature histories for straight channel cooling and conformal channel cooling

The difference between two cases shown in Figure 2 has to do with the rate of the energy transfer into the mold over successive injections and the thermal inertia of the mold. As the hot plastic comes in during each successive injection, heat transfer takes place across the plastic mold interface and a heat pulse is conducted through the mold material itself. This heat pulse warms up the mold material as it propagates toward the cooling channels and is eventually

removed in the cooling water. If the cooling channels are far from the mold's surface, successive heat pulses keep raising the temperature of the mold until the heat pulse propagating in is balanced by heat extraction by the coolant. If the cooling channels are close to the mold surface, the effective thermal mass of the tool is confined to that region between the surface and the cooling channels and is much reduced. In addition, the conduction path from the surface of the tools to the cooling lines is reduced. As a result, the steady state condition is reached much more rapidly and can in fact be attained within one injection cycle.

An energy balance may be written for the active portion of the mold, that is the portion between the surface and the cooling lines. Equation (1) shows the resulting differential equation (see Appendix A for derivation of this equation).

$$\rho_m C_m l_m \frac{dT_m}{dt} + \frac{h\pi D K_m}{2K_m W + h\pi D l_m}(T_m - T_c) = \frac{\rho_p C_p l_p (T_{melt} - T_{eject})}{t_{cycle}} \qquad (1)$$

The first term in Equation (1) captures the thermal mass of the tool and the build-up of heat as the temperature of the tool increases. The second term in Equation (1) captures the transfer of heat by conduction through the mold and then convection into the cooling fluid. The right hand side of Equation (1) captures the source of the heat, which is the cooling down of the plastic. This first order differential ordinary differential equation has the solution of the form shown in Equation (2) where T_{ms} is the cycle averaged mold temperature at steady state and τ is the time constant of the system. Equations (3) and (4) give the expressions for cycle averaged mold temperature and the time constant respectively. Our definition of conformal cooling can now be stated formally by requiring that τ be less than or equal to one injection cycle time. Figure 3 shows a prediction of Equation (2) superimposed on the experimental results previously shown in Figure 2. As can be seen, there is reasonably good prediction with the cycle average temperature.

$$T_m(t) = T_{m0} + (T_{ms} - T_{m0})e^{-t/\tau} \qquad (2)$$

$$T_{ms} = T_c + \frac{\rho_p C_p l_p (2K_m W + h\pi D l_m)(T_{melt} - T_{eject})}{h\pi D K_m t_{cycle}} \qquad (3)$$

$$\tau = \frac{\rho^m C^m l_m (h\pi D l_m + 2K^m W)}{h\pi D K^m} \qquad (4)$$

A limiting case of Equation (4) is that where the heat transfer to the fluid is very efficient and we can then examine the limiting case where the heat transfer coefficient goes to infinity. In this case, the expression for the time constant reduces to the form shown in Equation (5). In this simplified expression we see that the important material property for the mold is the thermal diffusivity which is $K_m / \rho_m C_m$. We also see that the time constant is proportional to the square of the distance between the surface of the mold and the cooling channels. This simplified expression makes clear the importance of considering this as a transient heat transfer calculation. If this were a steady state heat transfer problem then doubling the thermal conductivity of the

mold would allow the channels to be placed twice as far away. However, as we can see from Equation (5) if we double the thermal conductivity and place the channels twice as far away the time constant in fact increases by a factor of 2. Thus, while the material properties are important, the geometry (as seen by the square of the distance of Equation (5)) is even more important.

$$\tau = \frac{\rho_m C_m l_m^2}{K_m} \tag{5}$$

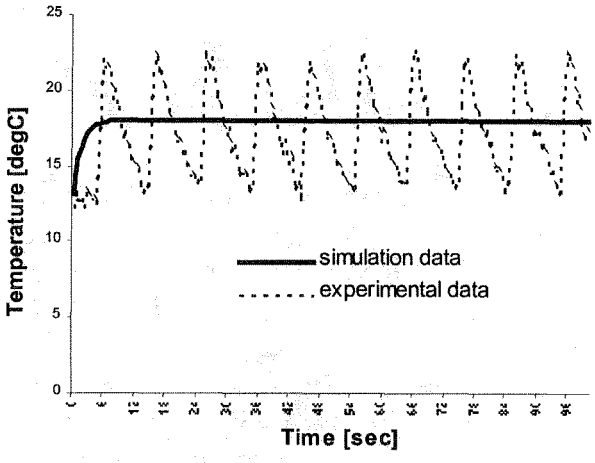

Figure 3. Comparison of the experiment data vs. the simulation data for the mold surface temperature profile during successive injections

3. Design methodology

The introduction of conformal cooling significantly simplifies the injection molding cooling system design methodology. In the conformal cooling situation, the heat transfer is localized in a small region between two adjacent cooling channels. This feature suggests that we first design a cooling "cell" composed of the small region between the adjacent cooling lines and then map the solution to the entire mold. The flexibility of SFF processes makes this modular approach possible by minimizing the manufacturing constraint that must be applied. This strategy simplifies the cooling line design by providing a sequential approach which provides a global solution by the addition of many local solutions. While the design process is simplified, the resulting cooling line designs can be quite complex and take full advantage of the flexibility of SFF processes.

Figure 4 illustrates this design strategy by using a generic part with a hemispherical dome and a flat bottom. As shown in the figure, the part is first divided into two cooling zones (a hemisphere and a flat surface) based on its geometry. Then in each cooling zone the conformal cooling surface is constructed and the cooling channel topological structure is defined. After that the system of cooling channels is further decomposed into small elements called cooling cells.

The heat transfer analysis and the cooling system design is based on these cooling cells and is then mapped to the entire mold. This modularized design strategy is not sensitive to the part geometry, therefore it keeps the same design simplicity no matter how complex the part geometry is.

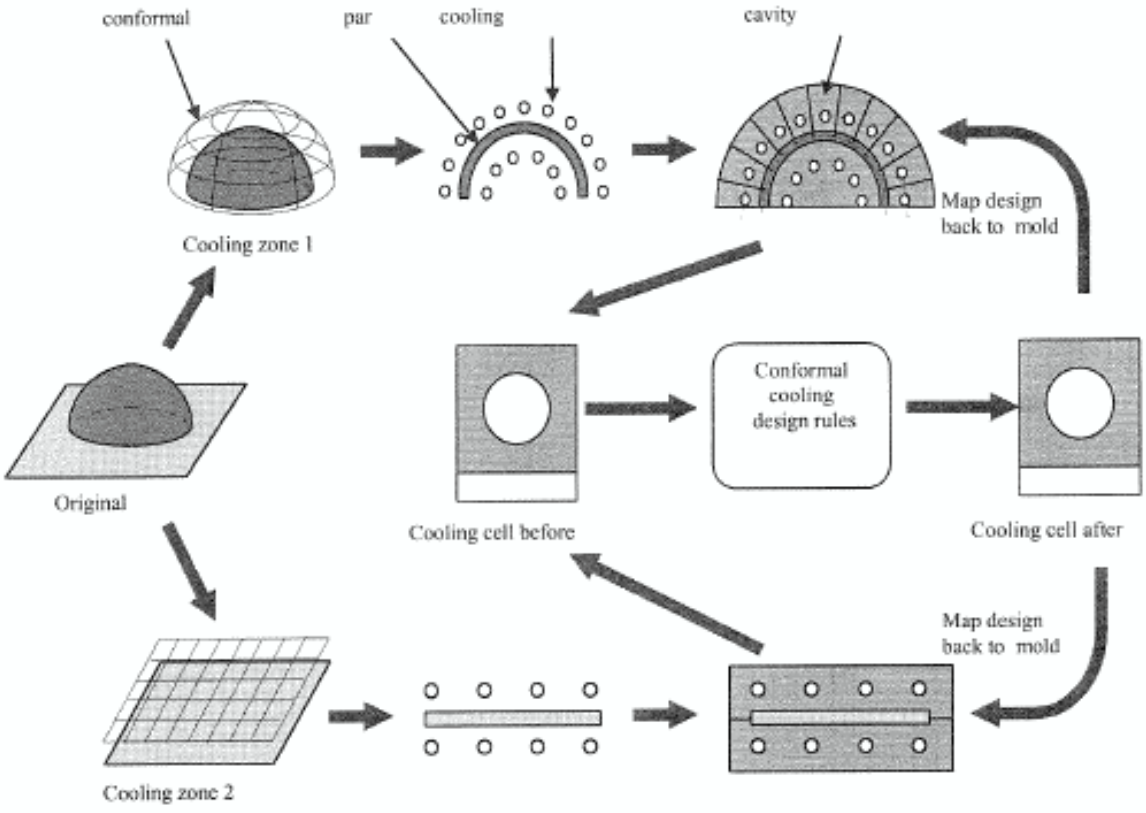

Figure 4 Steps for the modularized cooling line design for a generic part

4. Design rules

After the cooling system has been decomposed into simple cooling cells by the method discussed above, the design rules are applied to these cooling cells in order to obtain cooling channel design parameters and process conditions. In this chapter, six design rules are proposed and design windows are constructed for the cooling line design based on individual cooling cells. These rules include design for conformal cooling condition, design for coolant pressure drop, design for coolant temperature uniformity, design for sufficient cooling, design for uniform cooling and design for mold strength and deflection.

4.1 Design for conformal cooling condition

The conformal cooling condition defined in section 2 must be applied throughout the tooling in order to guarantee the good control of the temperature at the surface of the tool. In order to satisfy this condition, the mold designer can increase the heat transfer coefficient, increase the channel diameter, decrease the distance between the cooling lines and the mold wall

or choose mold material with a high thermal diffusivity. The determination of these design parameters is also constrained by other design rules that will be discussed below.

4.2 Design for coolant pressure drop

The allowable pressure drop of the coolant in the conformal cooling channel is constrained by the available pumping pressure of the chiller. The objective of the cooling line design for pressure drop is to find a proper combination of the coolant flow rate, the cooling channel diameter and the cooling line length so that the resulting total pressure drop is smaller than the given pressure budget. The fluid mechanics of the incompressible flow can be used to predict the coolant pressure drop that is a function of the cooling line length, the cooling line diameter and the coolant flow rate [27].

$$P = \frac{L}{2D}\rho v^2 C_f \tag{6}$$

where C_f in Equation (6) is the cooling channel surface friction factor which differs for different flow regions:

$$C_f = \frac{16}{R_{eD}} \quad \text{(for laminar flow)} \tag{7}$$

$$C_f = \frac{0.25}{1.8^2}\left(\log_{10}\left[\left(\frac{e}{3.7D}\right)^{1.11} + \frac{6.9}{R_{eD}}\right]\right)^{-2} \quad \text{(for turbulent flow)} \tag{8}$$

In the above equations, R_{eD} is the Reynolds number of the coolant flow. e is the surface roughness of cooling channels.

4.3 Design for coolant temperature uniformity

The objective of the design for the coolant temperature uniformity is to check and make sure that the coolant temperature drop is maintained within a certain range. A simple expression of the coolant temperature drop ΔT is obtained by the following equation:

$$\Delta T = \frac{\rho_p C_p l_p w L}{\rho_c C_c Q} \cdot \frac{(T_{melt} - T_{eject})}{t_{cycle}} \tag{9}$$

where l_p is half the plastic part thickness, w is the cooling line pitch distance, L is the cooling line length, Q is the coolant flow rate and t_{cycle} is the injection cycle time. ρ_c, C_c, ρ_p, C_p are the densities and specific heats for coolant and part materials respectively. Equation (9) indicates that during the steady injection cycles the heat pulse due to the cooling down of the plastic part is totally converted to the temperature rise of the coolant flow. In order to reduce the coolant temperature drop, the designer can use the coolant with large thermal mass, increase the coolant flow rate, decrease the pitch distance between two adjacent cooling channels or reduce the length of the cooling line.

4.4 Design for sufficient cooling

As we have discussed in section 1, the cooling analysis scheme adopted by most of mold design software is computationally expensive and not good for the design and analysis of complex cooling channels. With the concept of conformal cooling, this scheme is much simplified. As the matter of fact, the steady cycle averaged mold temperature can be directly derived from Equation (3). However, this expression requires both the part ejection temperature T_{eject} and the cycle time t_{cycle} which can not be both obtained. A simple iteration discussed below finds the cycle time and the steady cyclic mold temperature T_{ms} based on the required part ejection temperature:

Step 1. Assume the cycle averaged mold temperature T_{ms}.
Step 2. Calculate the cycle time t_{cycle} for the required part ejection temperature according to 1D part heat transfer.
Step 3. Calculate the part ejection temperature at the end of t_{cycle}.
Step 4. Calculate the cycle averaged mold temperature T_{ms} based on equation (3).
Step 5. Replace T_{ms} in step 1 by the cycle averaged mold temperature value obtained in step 4.
Step 6. Follow the iterations from step 1 to 5 until the cycle averaged mold temperature T_{ms} reaches a steady value.

For readers with special interest in detail algorithms, please refer to Appendix B.

4.5 Design for uniform cooling

The "uniform cooling" in this paper has both the global and the local meanings. The global uniformity is the cooling rate variation over the entire mold. It is guaranteed by keeping the coolant temperature uniformity. The local cooling uniformity refers to the variation of the mold surface temperature within the individual cooling cell sketched in Figure 5(a). The local cooling uniformity is defined by the difference of the cycle averaged temperatures on the mold surface right above the cooling channel and at the middle of two adjacent channels, i.e. points A and B in Figure 5(a).

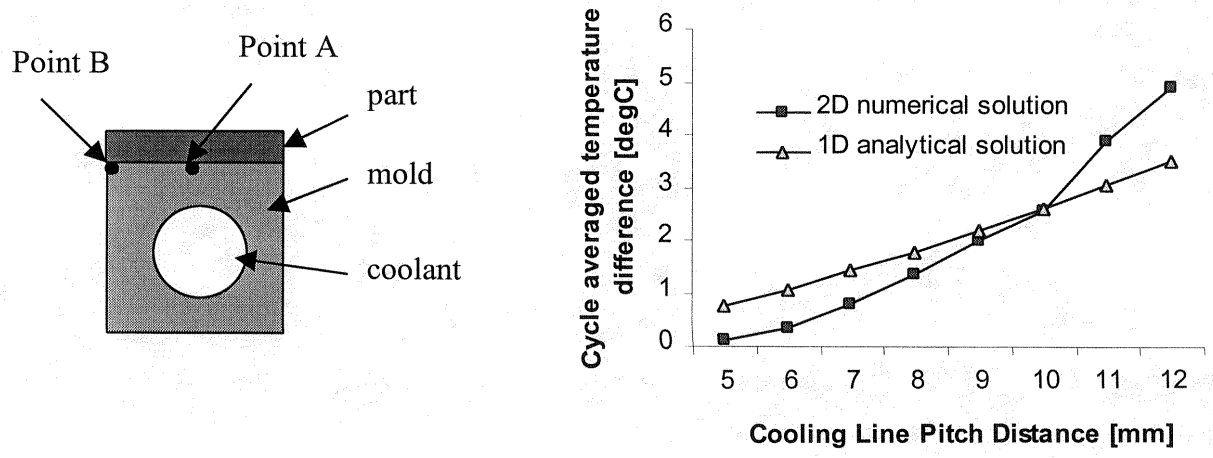

(a) (b)

Figure 5 (a) Sketch of a cooling cell for cooling uniformity analysis. (b) Comparison of the analytical and numerical solutions for cycle averaged mold surface temperature differences at point A and B

The cycle averaged mold surface temperatures at point A and point B are expressed by the following equations:

$$T_{ma} = T_c + \frac{\rho_p C_p l_p (2K_m W + h\pi D l_a)(T_{melt} - T^a_{eject})}{h\pi D K_m t_{cycle}} \tag{10}$$

$$T_{mb} = T_c + \frac{\rho_p C_p l_p (2K_m W + h\pi D l_b)(T_{melt} - T^b_{eject})}{h\pi D K_m t_{cycle}} \tag{11}$$

where l_a and l_b are the depth of the heat diffusion into the mold at point A and point B respectively. T^a_{eject} and T^b_{eject} are part ejection temperatures at A and B respectively. The cycle averaged temperatures T_{ma} and T_{mb} are obtained following the same routine as discussed in section 4.4. The local cooling uniformity of the mold is thereby defined as the absolute value of the cycle averaged temperature difference between point A and point B:

$$\Delta T_{ab} = | T_{ma} - T_{mb} | \tag{12}$$

Figure 5(b) plots the local cooling uniformity and compare it with the numerical solution (see Appendix C for details) for different cooling line pitch distance. The material properties used for this calculation are those of polystyrene (part), 316 stainless steel (mold) and 30 °C water (coolant). The calculation is based on 2mm part thickness, 4mm cooling channel diameter and 3mm vertical distance from cooling line to mold wall. The heat conduction distances l_a and l_b in equation (19) and (20) are chosen to be distances from point A and B to the wall of the cooling channel respectively. As one can see from the figure, the analytical and numerical solutions match very well in a certain pitch distance range. More accurate prediction can be achieved by adding adjustment factors to l_a and l_b.

4.6 Design for mold strength and deflection

Rao [3] predicted the mold stress and delection based on the rectangular cooling channel model shown in Figure 6. According to his model, the maximum tensile stress in the mold under a certain injection pressure P_m is:

$$\sigma_{\max} = \frac{0.5 P_m D^2}{l_m^2} \tag{13}$$

The maximum shear stress in the mold is:

$$\tau_{\max} = \frac{0.75 P_m D}{l_m} \tag{14}$$

The maximum mold surface deflection under pressure P_m is:

$$f_{\max} = \frac{P_m D^2}{l_m}\left(\frac{D^2}{32E_m l_m^2} + \frac{0.15}{G}\right) \tag{15}$$

The above expressions represent the worst case of the loading because the commonly used cooling channels are circular shaped that result in much smaller stress and deflection. The numerical simulation shows that the stress concentration is reduced by over 50% if we choose channels with round corners.

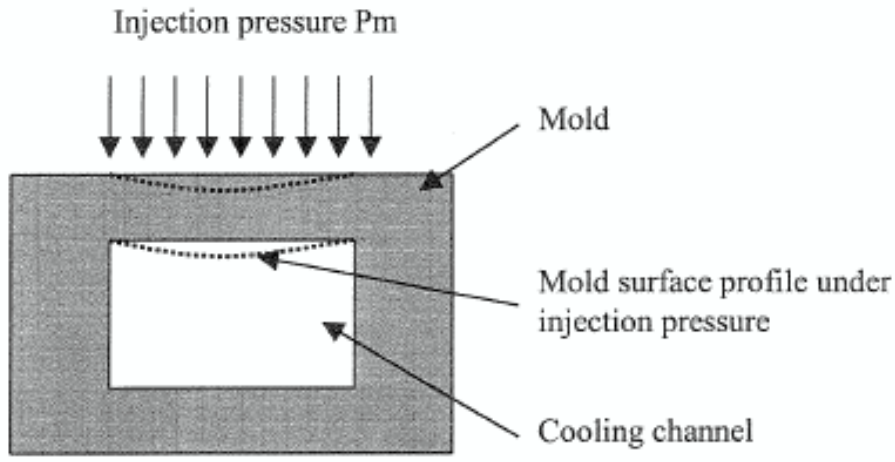

Figure 6 Sketch of a cooling cell under the injection pressure

5. Tool design and fabrication with conformal cooling channels

With the help of the conformal cooling line design methodology, the 3D Printing Lab of MIT has successfully designed and fabricated the mold inserts for the part shown in Figure 7. The challenge placed by this part is that the geometric features are so small and so close to each other that it gives the designer little room for the cooling channel placement. In order to proceed the conformal cooling line design for this part, we first divide the part into two cooling zones. For each cooling zone, the cooling line topological structure is defined and different cooling channel cross section shapes are assigned to different sections of the cooling line. Then the cooling system is further decomposed into individual cooling cells and the design rules are applied to these cells to obtain the local solution of the cooling channel parameters. The 2D numerical simulation (see Appendix C for details) is also used for the evaluation of the transient heat transfer in each cooling cell. Figure 9 shows the design results for individual cooling cells. These results include the cooling channel geometry, process condition as well as the evaluation of design rules such as the part ejection temperature, the coolant pressure drop, the mold stress, etc. In addition to the local design of individual cooling cells, the designer is responsible for coordinating between local solutions for the proper global performance. One example of such coordination is to balance the coolant flows between cooling zones. In the table shown in Figure 8 the coolant pressure drops for each section of the cooling zone are summed up so that the total pressure drop through each cooling zone is obtained. In order to maintain the equal coolant flow

between two cooling zones, it is important to make the total pressure drop in each cooling zone as close as possible.

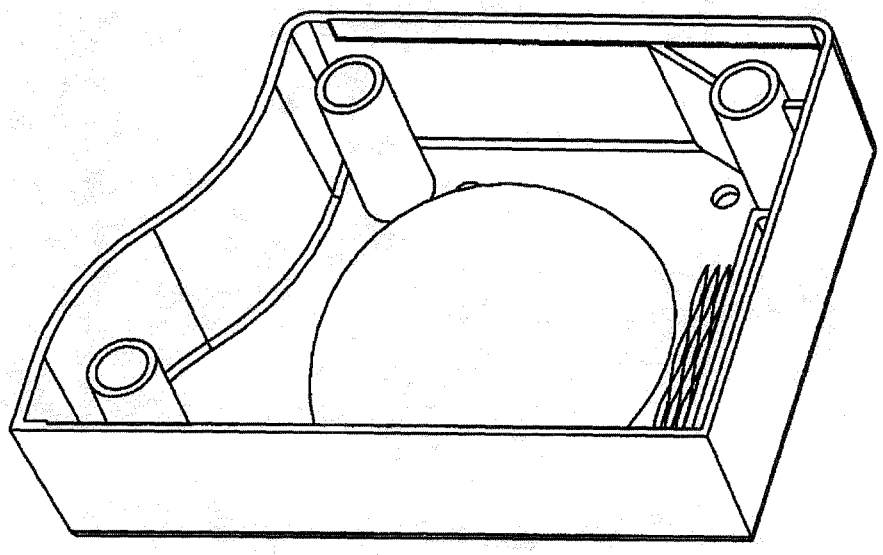

Figure 7 The part we used to demonstrate the conformal cooling design and fabrication ability

	Cooling zone 1		Cooling zone 2	
Cooling zone Topological Structure	1 2 3 section 1: inlet section 2: 3 parallel line section 3: outlet		1 2 3 section 1: inlet section 2: serpentine cooling lin section 3: outlet	
Section No.	1, 3	2	1, 3	2
Cross Section Shape	●	⬬	●	●
Hydraulic Diameter	6.35 mm	2.3 mm	8 mm	4 mm
Cooling Line Length	.03 m	.43 m	.03 m	1.15 m
Pitch Distance	10 mm	10 mm	10 mm	10 mm
Coolant Flow Rate	3 GPM	1 GPM	3 GPM	3 GPM
Reynolds	2800	36,000	2220	62,100
Coolant Pressure Drop	<<1psi	29.6 psi	<<1psi	37.5 psi
Total Pressure Drop	~ 30 psi		~38 psi	
Vert. Dist. To Mold Wall		2.5 mm		5 mm
Cooling Time		10 sec		10 sec
Max. Stress		< 13,000 psi		< 8094 psi
Part Ave. Temp.		62.95 degC		64.9 degC

Figure 8 Cooling system design results for the 3DP bench mark part

After the design parameters and process conditions for all the cooling cells have been determined, the solutions are mapped back to the entire mold to construct the global cooling system. Figure 1(b) shows the solid model of such a cooling system. The final tool with conformal cooling channels placed is obtained by subtracting the cooling system model from the mold insert and adding the manufacturing tolerance. The .stl file is then created for solid freeform fabrication. Figure 10 shows the resulting green part fabricated by 3D Printing process.

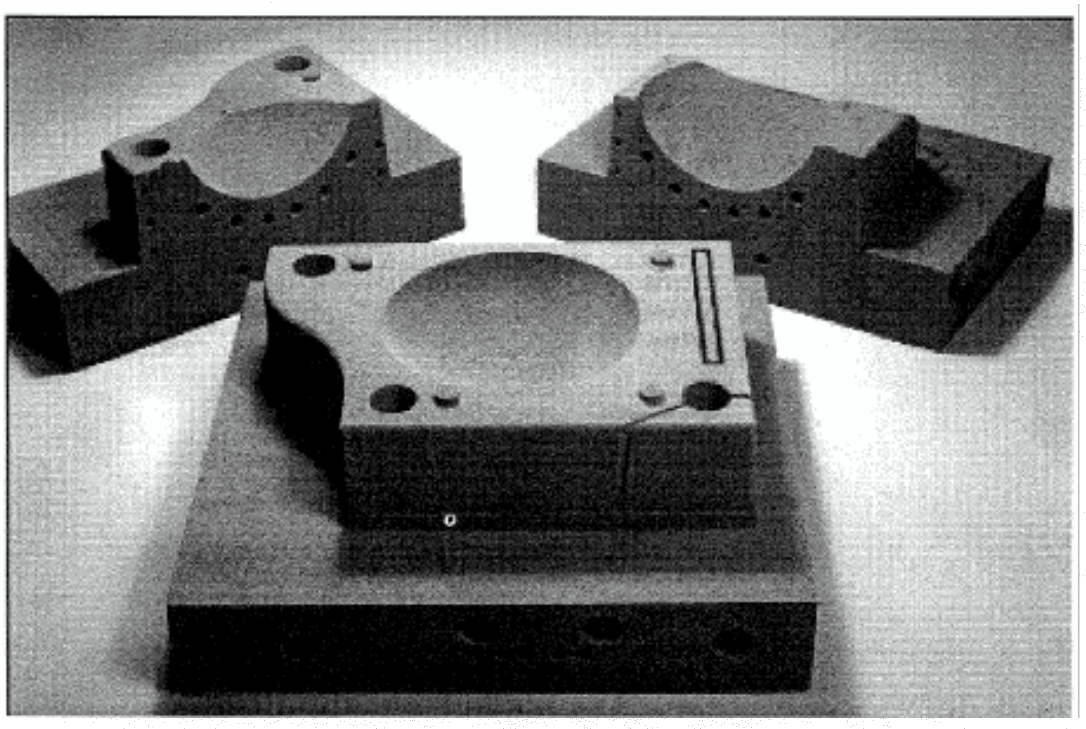

Figure 9 Green part of the insert fabricated by 3D Printing process based on the solid model in Figure 1

6. Conclusions

Solid Freeform Fabrication processes such as 3D Printing can create injection molding tooling with complex cooling channels offering the potential for substantial improvement in production rate and part quality. This capability raises the challenge of designing the complex cooling channels required to realize these improvements.

This work presents a systematic method for the design of cooling channels for tooling. First the mold surface is decomposed into manageable sections called cooling zones. Then a system of cooling channels is designed for each cooling zone. This system of cooling channels is further decomposed into smaller elements called cooling cells that are easy to analyze. The cooling cell is a sandwich structure covering the part, the mold and the cooling channel region between two adjacent cooling lines. Six design rules are applied in order to create design windows for the individual cooling cell. These design rules include design for conformal cooling condition, design for coolant temperature drop, design for part ejection temperature, design for

sufficient cooling, design for mold strength and deflection and design for cooling uniformity. After the design for individual cooling cell is finished, the solution is mapped back to the mold in order to build the entire conformal cooling system.

7. Acknowledgment

The work discussed in this paper is supported by the Technology Re-Investment Project, Cooperative Agreement (DMI - 9420964) funded by DARPA and administered by NSF, and the 3D Printing Industrial Consortium. The authors thank members of 3DP Consortium and the colleagues of 3DP Lab for their consistent support and encouragement. Special thanks are due to Dick Barlik from Hasbro, who designed the prototype part for the 3DP benchmark tool, David Brancazio and Jim Serdy from 3D Printing Lab of MIT, who took care of most of the work from administration to manufacturing of the conformal cooling project, Dr. K. K. Wang and Dr. Hieber from Cornell Injection Molding Program, who provided generous help and encouragement in mold cooling system design and simulation.

8. Nomenclature

ρ_m, ρ_p, ρ_c :	Density of the mold, the plastic part and the coolant
C_m, C_p , C_c :	Specific heat of the mold, the plastic part and the coolant
K_m , K_p , K_c :	Thermal conductivity of the mold, the plastic part and the coolant
α_m, α_p, α_c:	Thermal diffusion of the mold, the plastic and the coolant
μ_c :	Coolant viscosity
Re_D:	Coolant Reynolds number
Q:	Coolant flow rate
v:	Coolant flow velocity
h_c :	Heat transfer coefficient between mold and coolant
e:	Cooling channel surface roughness
C_f:	Cooling channel surface friction factor
T_{melt}:	Plastic melt processing temperature
T_{eject}:	Plastic ejection temperature
T_m^s :	Cycle averaged mold temperature at steady operation
$T_m(t)$:	Cycle averaged mold temperature as a function of time
T_m^s :	Cycle averaged mold temperature
T_c:	Coolant temperature
l_m:	Vertical distance from cooling line to mold wall
l_p:	Half the plastic part thickness
D:	Cooling channel diameter
w:	Cooling line pitch distance
L:	Cooling line length
E_m:	Young's modulus of the mold
G_m:	Shear modulus of the mold
Δm:	Step length of finite difference nodes for the mold
Δp:	Step length of finite difference nodes for the part
Δt:	Step length for the simulation time

t_{cycle}: Injection cycle time
τ: mold time constant

9. Reference

1. Z. Tadmore, C. Gogos, "Principles of Polymer Processing", Wiley, 1979, p584 - 610
2. R. Pye, "Injection mould design", Longman, 1989
3. N. Rao, "Design formulas for plastics engineers", Hanser, 1991, chapter 6
4. D. Rosato, "Injection Mold Design Handbook", Van Hostrand Reinhold Comp., NY, 1985, Chapter 7, p160 - 234
5. K. Singh, "Design of Mold Cooling System", *Injection and Compression Molding Fundamentals*, A. Isayev Ed., Marcel Dekker, 1991, p567 - 605
6. C. Austin, "Mold cooling", *ANTEC '85*, p764 - 768
7. E. Chu, M. Kamal, S. Goyal, "A Computer Simulation of the Injection Molding Process Including Filling, Packing and Solidification", *ANTEC'89*, p344 - 347
8. T. Kwon, "Application of the Boundary Integral Method to the Nonisothermal Flow of a Polymeric Fluid Advancing in a Thin Cavity of Arbitary Shape", *CIMP Technical Report*, No. 38 Jan-82
9. T. Kwon, "Mold Cooling System Design Using Boundary Element Method", *ASME Journal of Eng. for Industry*, Vol. 110, p384 - 394
10. L. Turng, "Application of the Boundary Element Method to the Cooling-Line Design for Injection Molds", *CIMP Technical Report*, No. 56, Jan-87
11. L. Turng, K. Wang, "A computer - aided cooling line design system for injection molds", *Journal of engineering for industry*, vol 112, May-90, p161
12. K. Himasekhar, J. Lottey, K. Wang, "CAE of Mold Cooling in Injection Molding Using a Three Dimensional Numerical Simulation", *Journal of Engineering for Industry*, vol. 114, May-92, p213 - 221
13. S. Chen, S. Yu, A. Davidoff, "Hybrid Mehods for Injection Mold Cooling Process Simulation and Mold Cooling System Analysis", *ANTEC'91*, p499 - 503
14. S. Hu, N. Cheng, S. Chen, "Effect of Cooling System Design and Process Parameters on Cyclic Variation of Mold Temperatures - Simulation by DRBEM", *Plastics, Rubber and Composites Processing and Applications*, Vol. 23, No. 4, 1995, p221 - 231
15. M. Rezayat, T. Burton, "Combined Boundary-Element and Finite - Difference Simulation of Cooling and Solidification in Injection Molding",
16. Y. Lauze, J. Hetu, "Temperature Prediction of Part and Mold Using Finite Element Simulations", *ANTEC'94*, p809 - 812
17. M. Rezayat, "Numerical Computation of Cooling-Induced Residual Stress and Deformed Shape for Injection-Molded Thermoplastics", *ANTEC'89*, p341 - 343
18. R. Thomas, N. McCaffery, "The Prediction of Real Product Shrinkage Calculated from a Simulation fo the Injection Molding Process", *ANTEC'89*, p371 - 375
19. S. Chen, N. Cheng, K. Jeng, "Post-Filling Simulation and Analyses of Shrinkage and Warpage of the Injection Molded Parts", *ANTEC'91*, p493 - 498
20. G. Titomanlio, K. Jansen, "In-Mold Shrinkage and Stress Prediction in Injection Molding", *Polymer Engineering and Science*, Vol. 36, No. 15, Aug-96, p2041 - 2049

21. S. Liu, "Modeling and Simulation of Thermally Induced Stress and Warpage in Injection Molded Thermoplastics", *Polymer Engineering and Science*, Vol. 36, No. 6, Mar-96, p807 - 818
22. W. Zoetelief, L. Douven, A. Housz, "Residual Thermal Stresses in Injection Molded Products", *Polymer Engineering and Science*, Vol. 36, No. 14, Jul-96, p1886 - 1896
23. H. L. Marcus, D. L. Bourell, "Solid Freeform Fabrication Finds New Applications", Advanced Materials & Processes, Sept – 1993, p28 - 35
24. E. Sachs, M. Cima, P. Willams, D. Brancazio, J, Cornie, "Three dimensional printing: rapid tooling and prototypes directly from a CAD model", *Transactions of the ASME: Journal of Engineering for Industry*, vol 114, no.4, Nov -1992, p481 - 488
25. E. Sachs, E. Wylonis, M. Cima, S. Allen,S. Micheals, E. Sun, H. Tang, H. Guo, "Injection Molding Tooling by Three Dimensional Printing: a Desktop Manufacturing Process", *ANTEC'95*
26. E. Sachs, S. Allen, H. Guo, J. Banos, M. Cima, J. Serdy, D. Brancazio, "Progress on Tooling by 3D Printing: Conformal Cooling, Dimensional Control, Surface Finish and Hardness", Solid Freeform Fabrication Proceedings, Sept-1997, p115-123
27. J. Fay, *Introduction to Fluid Mechanics*, MIT Press, 1995
28. Mills, *Heat and Mass Transfer*, Irwin Press, Chicago, 1995